EFFECT OF BONDING ON THE PERFORMANCE OF A PIEZOACTUATOR-BASED ACTIVE CONTROL SYSTEM

by

A.Baz
Mechanical Engineering Department
The Catholic University of America
Washington, D.C. 20064

S.Poh
Mechanical Engineering Department
The Catholic University of America
Washington, D.C. 20064

ACKNOWLEDGEMENTS

Special thanks are due to the Space Science and Technology branch at NASA Goddard Space Flight Center for providing the funds necessary to conduct this study under grants number NAG-520 and NAG-749.

Thanks are particularly due to Dr. Joseph Fedor, code 712, for his invaluable engineering inputs which have been crucial to the implementation of this effort.

Special thanks are also due to Mr. Eric Osborne, code 716, for his continuous thought stimulating discussions.

NOMENCLATURE

b	width of beam and piezo-actuator, m
d	electric charge constant of piezo-actuator, m/v
D	distance to neutral axis of composite beam measured from its lower edge, m
$E_{1,2,3}$	Young's modulus of elasticity of piezo-actuator and beam respectively, N/m^2
E_i	Young's modulus of elasticity of element i of the beam, N/m^2
f	vector of modal forces and moments, N or Nm
F	vector of external forces and moments, N or Nm
$I_{1,2,3}$	area moment of inertia of actuator, bonding layer and beam about the neutral axis of the composite beam respectively, m^4
I_i	area moment of inertia of the element i, m^4
J_i	mass moment of inertial of the composite beam at node i, $kg\text{-}m^2$
K_i	stiffness matrix of the element i
K	overall stiffness matrix of beam-actuator system
L_i	length of element i, m
m_i	mass of the composite beam at node i, kg
M	mass matrix of beam-actuator system
M_{ei}	external moment acting on i^{th} node of beam, Nm
M_f	piezo-electric moment generated by piezo-film, Nm
N	number of elements of the beam
$t_{1,2,3}$	thickness of piezo-actuator, bonding layer and beam respectively, m
U	modal coordinates of the flexible system
v	voltage applied across the piezo-electric film, volts

V_i external force acting on the i^{th} element of the beam, N

y_i the linear translation of node i, m

$w_{b,f,s}$ bond, film and beam mass per unit length respectively, kg/m

Greek Letters

γ_i factor=1 or zero if actuator is bonded to element i or not respectively

δ_i deflection of node i, m or rad.

δ deflection vector of all nodes of the beam, m or rad.

$\ddot{\delta}_i$ acceleration vector of all nodes of the beam, m/s^2 or rad/s^2

ϵ_f piezo-electric strain in piezo-actuator, m/m

θ_i angular deflection of node i, rad.

λ diagonal matrix of the eigenvalues of the system

$\sigma_{1,2,3}$ bending stresses in piezo-actuator, bonding layer and beam respectively, N/m^2

σ_f piezo-electric stress in actuator, N/m^2

ϕ modal shape matrix of the eigenvectors of the flexible system

SUMMARY

This study deals with the utilization of piezo-electric actuators in controlling the structural vibrations of flexible beams.

A Modified Independent Modal Space Control (MIMSC) method is devised to select the optimal location, control gains and excitation voltage of the piezo-electric actuators in a way that would minimize the amplitudes of vibrations of beams to which these actuators are bonded, as well as the input control energy necessary to suppress these vibrations.

The presented method accounts for the effects that the piezo-electric actuators and the bonding layers have on changing the elastic and inertial properties of the flexible beams.

Numerical examples are presented to illustrate the application of the MIMSC method and to demonstrate the effect of the physical and geometrical properties of the bonding layer on the dynamic performance of the actively controlled beams.

The obtained results emphasize the importance of the devised method in designing more realistic active control systems for flexible beams, in particular, and large flexible structures in general.

INTRODUCTION

Active vibration control systems are becoming essential and viable means for minimizing the vibrations of large flexible structures which are intended to provide stable bases for precision pointing in space.

Distinct among the presently available active control systems are those that rely in their operation on piezo-electric actuators. Such systems have proven to be experimentally effective in controlling the vibrations of simple structural elements such as rectangular beams [1-2] and hollow cylindrical masts [3]. The effectiveness of these systems is coupled also with the light weight, high force and low power consumption capabilities of the piezo-electric actuators [4-8]. These features rendered this class of actuators to be an attractive candidate for controlling structural vibrations.

The present state-of-the-art of this type of actuators has been limited to the analysis and testing of their characteristics [9-11] as influenced by their geometrical or operational conditions. A recent attempt has been made by Baz [12], to select their optimal geometrical parameters and location which are best suited for a particular structure subjected to known static loading conditions. The developed synthesis procedure has proven to be essential to the successful integration of the actuators into the structure in order to minimize its static deformation.

However, no effort has been done to optimize the control of the vibrations of a multi-mode flexible system using a small number of optimally placed piezo-actuators through the development of efficient and realistic control algorithm that ensures minimal amplitudes of oscillation and input control energy.

It is, therefore, the purpose of this study is to devise such an optimal control method that is based on a modification of the well known Independent Modal Space Control(IMSC) method [13-15]. The devised method accounts for the spillover from the controlled modes into the uncontrolled modes due to the use of fewer actuators than the modeled modes. The developed method incorporates also an optimal placement procedure that will enable the selection of the optimal location of the piezo-electric actuators in the structure in order to guarantee a balance between the suppression of the amplitudes of vibration and the input control energy [16].

Furthermore, the developed procedure considers the effect that the piezo-electric actuators and bonding layers have on changing the elastic and inertial properties of the structure to which they are bonded to. Such changes result in modifying the normal modes of the structure one way or another depending on the physical and geometrical properties of the actuators and the bonding layers.

In this study, the emphasis will be placed on piezo-electric actuator-beam systems to illustrate the devised control strategy. But, without any further modifications, the developed method can be readily applied to large structures.

THE PIEZO-ELECTRIC ACTUATOR-BEAM SYSTEM

A. GENERAL LAYOUT

Figure (1) shows a general layout of a flexible beam (A) whose deflection is to be controlled by piezo-electric actuator (B) bonded to the beam by bonding layer (C). The beam, under consideration, can

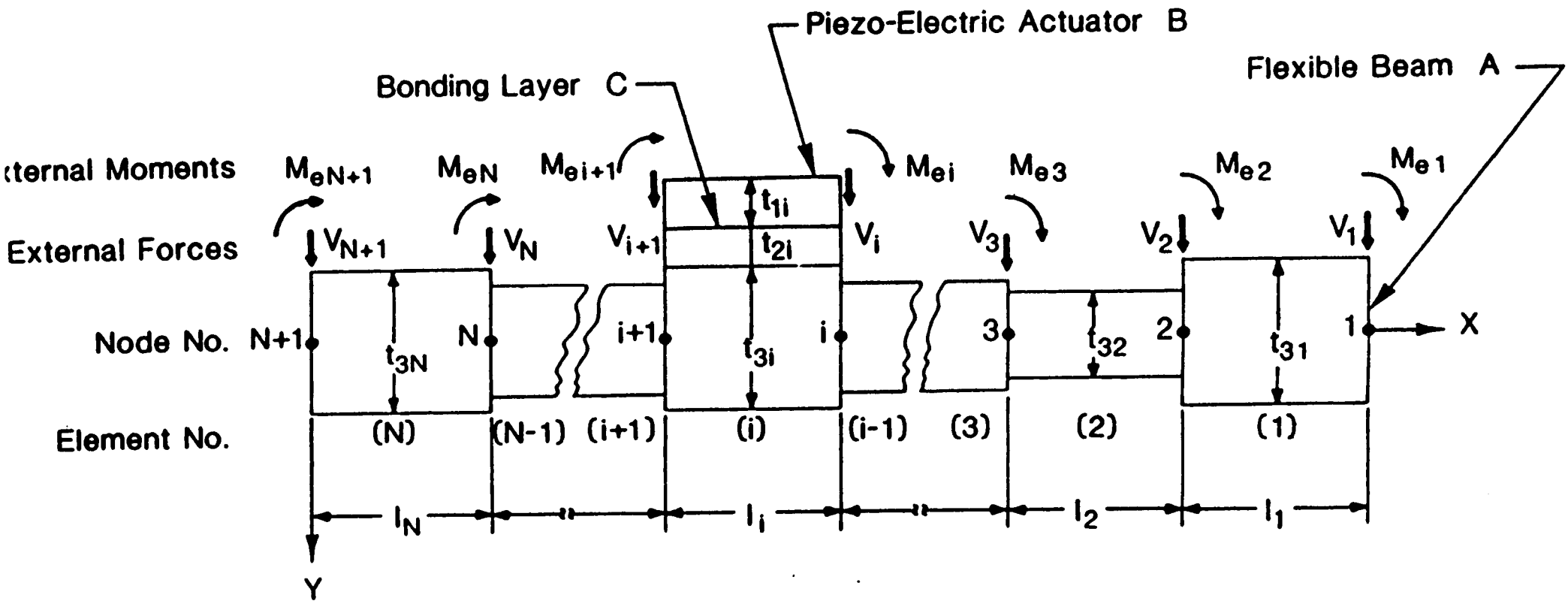

Figure (1) - General layout of the piezo-electric actuator-beam system.

generally be made of several steps which are not necessarily of the same thickness or the same material. The interfacial nodes between the different steps can be subjected to external forces, moments or both. Further, the degrees of freedom of any node can be limited to linear translations, angular rotations or restrained completely depending on the nature of support at the node under consideration.

In this study, the beam is assumed to have rectangular cross section of constant width b and that its transverse deflection is due to the flexural action of the external forces and moments.

In Figure (1), the piezo-electric actuator B is shown bonded to the element i of the flexible beam to form a composite beam. When an electric field is applied across the film, then it will expand if the field is, for example, along the polarization axis of the film and will contract if the two were out of phase. The expansion or contraction of the film relative to the beam, by virtue of the piezo-electric effect, creates longitudinal bending stresses in the composite beam which tend to bend the beam in a manner very similar to a bimetallic thermostat.

With proper selection, placement and control of the actuator, it would be possible to generate enough piezo-electric bending stresses to counter balance the effect of the exciting forces and moments acting on the beam in a way that minimizes its structural vibrations.

B. MODEL OF AN ACTUATOR-BEAM ELEMENT

Figure (2) shows a schematic drawing of a piezo-film A bonded to an element B of the flexible beam by bonding layer C.

If a voltage v is applied across the film, a piezo-electric strain ϵ_f is introduced in the film and can be computed from :

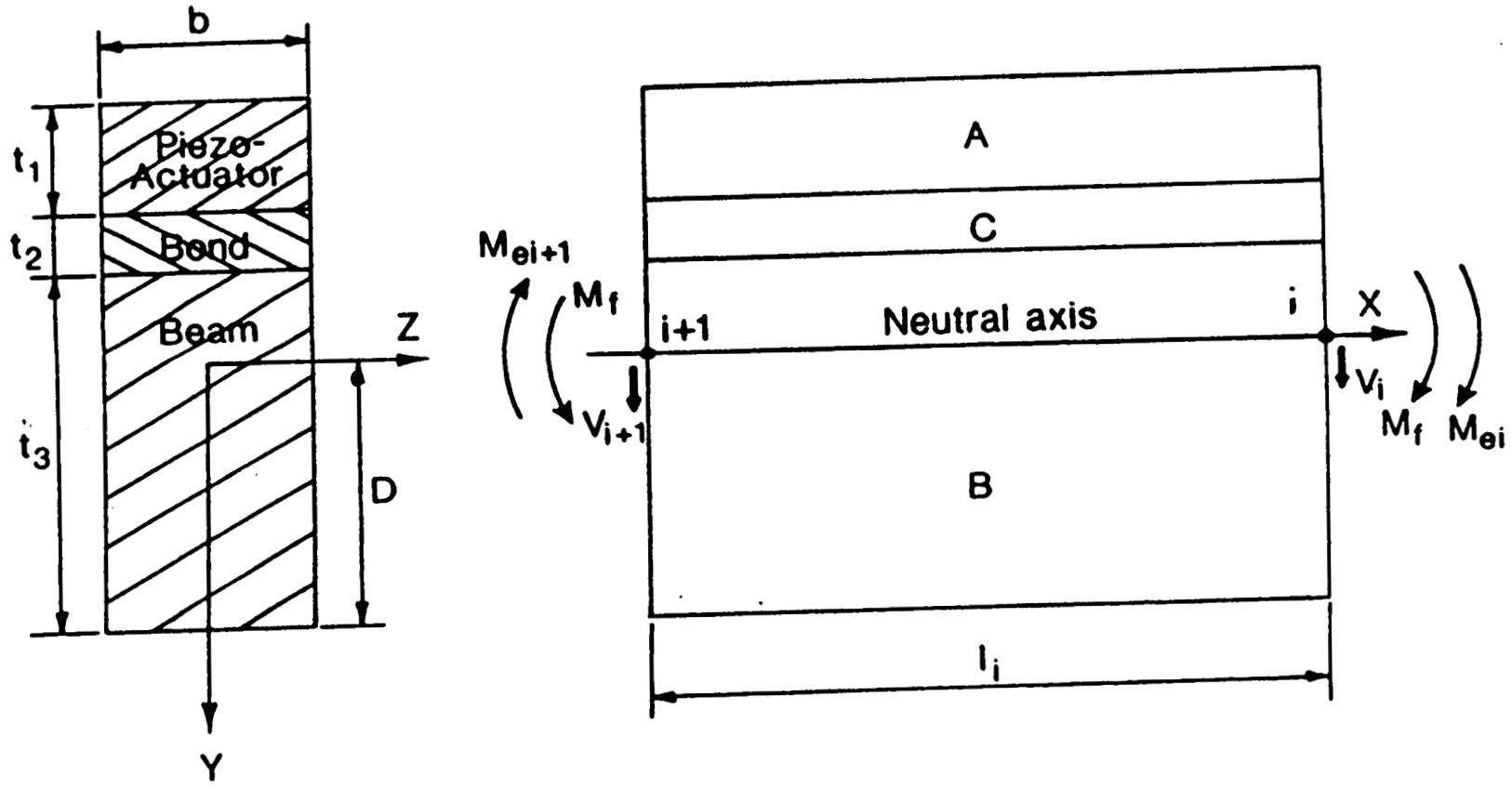

Figure (2) - Schematic drawing of an actuator bonded to a flexible beam element.

$$\epsilon_f = (d/t_1)*v \tag{1}$$

where d is the electric charge constant of the film, m/v

t_1 is the thickness of the piezo-electric actuator, m

This strain results in a longitudinal stress σ_f given by :

$$\sigma_f = E_1(d/t_1)*v \tag{2}$$

where E_1 is the Young's modulus of elasticity of the film, N/m^2

This, in turn generates a bending moment M_f, around the neutral axis of the composite beam, given by :

$$M_f = \int_{-(t_2+t_3-D)}^{-(t_1+t_2+t_3-D)} \sigma_f(b*y)dy \tag{3}$$

where t_2 is the thickness of the bonding layer, m

t_3 is the thickness of the beam, m

b is the width of the beam, the bonding layer and the piezo-film, m

In equation (3), D is the distance of the neutral axis from the lower edge of the beam which can be determined by considering the force balance in the longitudinal direction X of the beam, or :

$$\int_{film}\sigma_1 dA + \int_{bond}\sigma_2 dA + \int_{beam}\sigma_3 dA = 0 \tag{4}$$

or

$$E_1 b\int_{-(t_1+t_2+t_3-D)}^{-(t_2+t_3-D)} ydy + E_2 b\int_{-(t_2+t_3-D)}^{-(t_3-D)} ydy + E_3 b\int_{-(t_3-D)}^{D} ydy = 0 \tag{5}$$

where E_2 is Young's modulus of elasticity of the bonding layer

E_3 is Young's modulus of elasticity of the beam

Equation (5) yields the following expression for D :

$$D = \frac{E_1t_1^2+E_2t_2^2+E_3t_3^2+2E_1t_1(t_2+t_3)+2E_2t_2t_3}{2(E_1t_1+E_2t_2+E_3t_3)} \tag{6}$$

Equation (2), (3) and (6) can be combined to determine the bending moment M_f generated by the piezo-film on the composite beam as follows :

$$M_f = \frac{d*b*E_1*v*(E_2t_1t_2+E_3t_1t_3+E_2t_2^2+2E_3t_2t_3+E_3t_3^2)}{2*(E_1t_1+E_2t_2+E_3t_3)} \tag{7}$$

For this composite beam, it can be easily shown [12] that it has a flexural rigidity (E_iI_i) given by :

$$E_iI_i = E_1I_1 + E_2I_2 + E_3I_3 \tag{8}$$

where I_1, I_2 and I_3 are the area moments of inertia of the film, the bonding layer and the beam about the neutral axis respectively.

Let us now assume that the composite beam, shown in Figure (2), extends a length l_i between two nodes (i) and (i+1). Further, it is assumed that the external forces V_i and V_{i+1} as well as the external moments M_{ei} and M_{ei+1} are acting on the beam at nodes i and i+1 respectively. Then, the resulting linear and angular deformations of the beam y_i and θ_i as well as y_{i+1} and θ_{i+1} at the nodes i and i+1, respectively, can be related to the loads acting on the element as follows [17] :

$$\begin{bmatrix} V_i \\ M_{ei}+M_f \\ V_{i+1} \\ M_{ei+1}-M_f \end{bmatrix} = \frac{E_iI_i}{L_i^3} \begin{bmatrix} 12 & 6L_i & -12 & 6L_i \\ 6L_i & 4L_i^2 & -6L_i & 2L_i^2 \\ -12 & -6L_i & 12 & -6L_i \\ 6L_i & 2L_i^2 & -6L_i & 4L_i^2 \end{bmatrix} \begin{bmatrix} y_i \\ \theta_i \\ y_{i+1} \\ \theta_{i+1} \end{bmatrix} \tag{9}$$

Equation (9) can be rewritten as :

$$F_i = K_i \delta_i \qquad (10)$$

where F_i is the resultant forces and moments vector acting on the beam element i, N

K_i is the stiffness matrix of the composite beam element i, N/m

δ_i is the deflection vector of the nodes bounding the beam element, m

Equation (9) constitutes the basic finite element model that relates the external loads (V and M_e) and piezo-electric moments (M_f) to the deflections (y and θ) of the element as a function of its elastic and inertial parameters.

The equation can be equally used for any element of the beam whether it has a piezo-film bonded to it or not. In the latter case, M_f is set to zero and flexural rigidity E_iI_i is set equal to that of the flexible beam element under consideration.

The force-displacement characteristics of the individual elements of the beam-actuator system, as given for element i by equation (9), are combined to determine the overall stiffness K of the beam system as shown in References [18-19] for example.

The inertial properties of the composite actuator-beam system are determined using the lumped mass method where the mass and rotational inertial of each element is distributed among the nodes bounding the element [20].

Therefore, the diagonal mass matrix M ($2n*2n$) for the actuator-beam system, shown in Figure(1), can be written as :

$$
M = \begin{bmatrix}
m_1 & 0 & \cdot & \cdot & \cdot & \cdot & \cdot & \cdot & \cdot & \cdot & \cdot & \cdot & \cdot & \cdot & \cdot & 0 \\
0 & J_1 & 0 & \cdot & \cdot & \cdot & \cdot & \cdot & \cdot & \cdot & \cdot & \cdot & \cdot & \cdot & \cdot & \cdot \\
0 & 0 & m_2 & 0 & \cdot & \cdot & \cdot & \cdot & \cdot & \cdot & \cdot & \cdot & \cdot & \cdot & \cdot & \cdot \\
\cdot & \cdot & 0 & J_2 & 0 & \cdot & \cdot & \cdot & \cdot & \cdot & \cdot & \cdot & \cdot & \cdot & \cdot & \cdot \\
\cdot & \cdot & \cdot & \cdot & \cdot & \cdot & \cdot & \cdot & \cdot & \cdot & \cdot & \cdot & \cdot & \cdot & \cdot & \cdot \\
\cdot & \cdot & \cdot & \cdot & \cdot & 0 & m_i & 0 & \cdot & \cdot & \cdot & \cdot & \cdot & \cdot & \cdot & \cdot \\
\cdot & \cdot & \cdot & \cdot & \cdot & \cdot & 0 & J_i & 0 & \cdot & \cdot & \cdot & \cdot & \cdot & \cdot & \cdot \\
\cdot & \cdot & \cdot & \cdot & \cdot & \cdot & \cdot & 0 & m_{i+1} & 0 & \cdot & \cdot & \cdot & \cdot & \cdot & \cdot \\
0 & \cdot & \cdot & \cdot & \cdot & \cdot & \cdot & \cdot & 0 & J_{i+1} & 0 & \cdot & \cdot & \cdot & \cdot & \cdot \\
\cdot & \cdot & \cdot & \cdot & \cdot & \cdot & \cdot & \cdot & \cdot & \cdot & \cdot & \cdot & \cdot & \cdot & \cdot & \cdot \\
\cdot & \cdot & \cdot & \cdot & \cdot & \cdot & \cdot & \cdot & \cdot & \cdot & \cdot & 0 & m_N & 0 & \cdot & \cdot \\
\cdot & \cdot & \cdot & \cdot & \cdot & \cdot & \cdot & \cdot & \cdot & \cdot & \cdot & 0 & J_N & 0 & \cdot & \cdot \\
\cdot & \cdot & \cdot & \cdot & \cdot & \cdot & \cdot & \cdot & \cdot & \cdot & \cdot & \cdot & 0 & m_{N+1} & 0 & \cdot \\
0 & 0 & \cdot & \cdot & \cdot & \cdot & \cdot & 0 & \cdot & \cdot & \cdot & \cdot & \cdot & 0 & J_{N+1} & \cdot
\end{bmatrix} \qquad (11)
$$

where $m_1 = [(w_s+\gamma_1 w_f+\gamma_1 w_b)*L_1]/2$

$J_1 = [(w_s+\gamma_1 w_f+\gamma_1 w_b)*L_1^3]/2$

$m_i = [(w_s+\gamma_{i-1} w_f+\gamma_{i-1} w_b)*L_{i-1}+(w_b+\gamma_i w_f+\gamma_i w_b)*L_i]/2$

$J_i = [(w_s+\gamma_{i-1} w_f+\gamma_{i-1} w_b)*L_{i-1}^3+(w_b+\gamma_i w_f+\gamma_i w_b)*L_i^3]/12$

$m_{N+1} = [(w_s+\gamma_N w_f+\gamma_N w_b)*L_N]/2$

$J_{N+1} = [(w_b+\gamma_N w_f+\gamma_N w_b)*L_N^3]/12$

$w_{b,f,s}$ = bond, film and beam mass per unit length respectively, kg/m.

γ_i = 1 if an actuator is bonded to beam element i.
0 if not.

The stiffness and mass matrices K and M are used to define the dynamic equations of motion of the actuator-beam system.

The equations of motion of the actuator-beam system can be written as follows :

$$M\ddot{\delta} + K\delta = F \qquad (12)$$

modes.

$\phi_i(l_j)$ is the modal shape at mode i and location l_j.

The above equation can be rewritten as :

$$\begin{bmatrix} f_C \\ f_R \end{bmatrix} = \begin{bmatrix} B_{CC} & B_{CR} \\ B_{RC} & B_{RR} \end{bmatrix} * \begin{bmatrix} F_C \\ F_R \end{bmatrix} \tag{17}$$

If only C modes are controlled with equal number of control forces F_C, then F_R=0 and equation (6) reduces to :

$$f_C = B_{CC}F_C \tag{18}$$

and

$$f_R = B_{RC}F_C \tag{19}$$

In the IMSC method, it is assumed that the control forces F_C will not contribute to the excitation of the residual higher order modes. Accordingly, it was assumed that there is no control spillover from the controlled modes into the uncontrolled modes. Mathematically, this means that the IMSC method assumes that f_R=0. This of course can only be true if the number of controlled modes is very large compared to the number of residual modes or when the residual modes are at much higher frequency band than the controlled modes. If these two conditions are not satisfied, then there will be considerable interaction between the controlled and residual modes.

The MIMSC method considers such interaction by calculating the optimal modal control forces $[f_C]$ using the IMSC close form solution of the Riccati Equation such that the control force f_i of the i^{th} mode, as given by [7], is :

$$f_i = -(g_1\omega_i u_i + g_2\dot{u}_i)/R \tag{20}$$

where R is a factor that weighs the importance of minimizing the vibration with respect to the control forces.

ω_i is the resonant frequency at the i^{th} normal mode.

u_i, $\dot{u}_i$ are the modal displacement and velocity respectively.

g_1, g_2 are the modal position and velocity feedback gains given by [13] as :

$$g_1 = -\omega_i R + ((\omega_i R)^2 + \omega_i{}^2 R)^{1/2} \tag{21}$$

$$g_2 = (2R\omega_i(-\omega_i R + ((\omega_i R)^2 + \omega_i{}^2 R)^{1/2}) + \omega_i{}^2 R)^{1/2} \tag{22}$$

Accordingly, the displacement u_i and velocity $\dot{u}_i$ at the i^{th} mode can be feedback and used along with equations (20), (21) and (22) to determine the modal control force f_i.

Once these forces are calculated, equation (7) is solved to give the physically applied control forces F_C as follows :

$$F_C = B_{CC}{}^{-1} * f_C \tag{23}$$

Then equation (8) is used to calculate the modal forces f_R that would excite the residual modes which are generated by the spillover from the controlled modes. Definitely these f_R are not equal to zero as originally assumed in the IMSC method.

Equations (14) can then be integrated with respect to the time to determine the modal displacements (u_i) and velocities ($\dot{u}_i$) which can, in turn, be used again to compute the modal forces f and so on.

From the modal displacements and velocities, the physical state (δ) of the flexible system can be determined from equation (13). A relationship can therefore be established between the physical state of the system and the physical control forces F_C applied to it.

The MIMSC method incorporates also an extremely important feature which is based on a "TIME SHARING" strategy of a small number of actuators in the modal space to control large number of modes.

In this strategy, the modes of vibrations of the flexible system are ranked according to their modal energy level. If C actuators are to be used, then these actuators will be dedicated, at any instant of time, to control the C modes that have the highest modal energy. In this way, the actuators will first attenuate the modal energy of the controlled modes. During that time the control spillover will excite the uncontrolled modes. When the modal energy of the uncontrolled modes starts exceeding that of the controlled modes, the actuators are switched to control these high energy modes in order to damp out their vibrations. Such time sharing of the actuators between the modes will eventually bring all these modes under control.

Figure (3) outlines a flowchart of the MIMSC method indicating the main steps of optimal placement and time sharing of the actuators as well as the consideration of the spillover between the controlled and residual modes.

NUMERICAL EXAMPLES

The application of the MIMSC method is illustrated by considering a three-element straight steel cantilever beam, shown in Figure (4), which is 0.0125m wide, 0.0021m thick and 0.15m long. A transverse impulsive loading of magnitude of 0.1N is applied at the free end of the beam for 1.0ms.

The effects of varying the thickness and material of the bonding

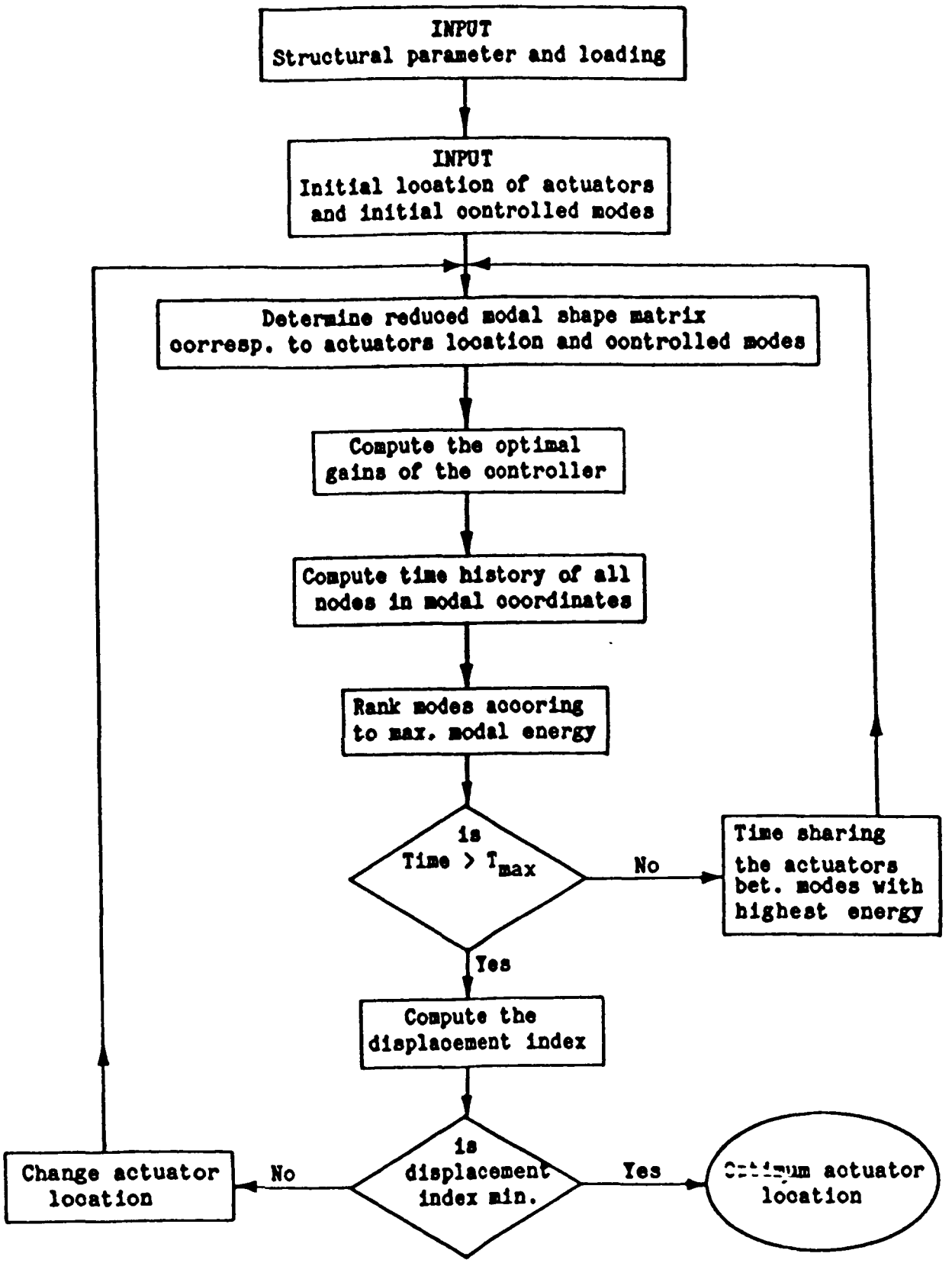

Figure (3) - Flowchart of the MIMSC algorithm

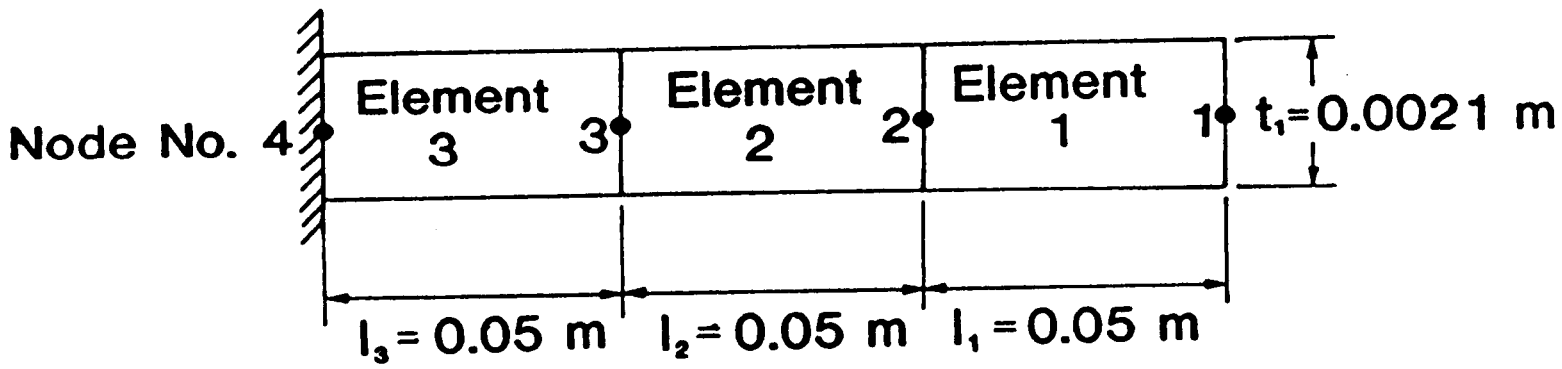

Figure (4) - Schematic drawing of a three-element cantilever beam

layer as well as the location of the piezo-actuator are considered.

The physical properties of the considered bonding layers and a typical piezo-actuator are given in Tables (1) and (2) respectively.

Figure (5-a) shows the time history of the amplitudes of transverse vibrations of the steel cantilever beam when controlled by the MIMSC method using one PZT piezo-electric actuator, bonded to the element near the fixed end of the beam. In this figure the effect of bonding layer on the physical properties of the system is neglected. The performance of the system under such conditions will serve as a datum for measuring the actual effect of the bonding layer when it is accounted for in the system's model.

With the time sharing concept, the MIMSC utilizes effectively the installed actuator such that it provides the necessary action to control the dominant modes and then shares the controller among the other modes until the vibrations of the system is completely damped out based on the maximum modal energy ranking. This time sharing concept can best be understood by considering Figures (5-b) and (5-c).

Figure (5-b) shows the control mode that has the highest modal energy at any instant of time. It can be seen that the actuator is used first to attenuate the amplitude of vibration of the first mode, which currently has the highest modal energy. After a small time interval the control action is switched to control the second mode since its modal energy becomes higher than the energy of the other five modes. This action of time sharing the single actuator between the modes continues until all modes are brought under control. This is demonstrated clearly in Figure (5-c) by the continuously decaying vibration energy of the system.

Table (1) - Properties of bonding layers [10]

Bonding Layer	Density (Kg/m^3)	Young's Modulus (MN/m^2)
Isotac[1]	890	1.1
Eastman 910[2]	1050	1780.0

1 Rubber adhesive tape made by Minnesota Mining and Manufacturing. St. Paul, Minn.
2 Cyanoacrylate adhesive made by eastman Kodak Co., Rochester, N.Y.

Table (2) - Properties of a typical piezo-electric actuator [8]

Material	PZT
Charge coefficient d 10^{-12} (m/v)	123
Young's modulus (G N/m^2)	139
Max. voltage v^* (Mv/m)	1
Max. tensile strength σ^* (M N/m^2)	45
Density (kg/m^3)	7500

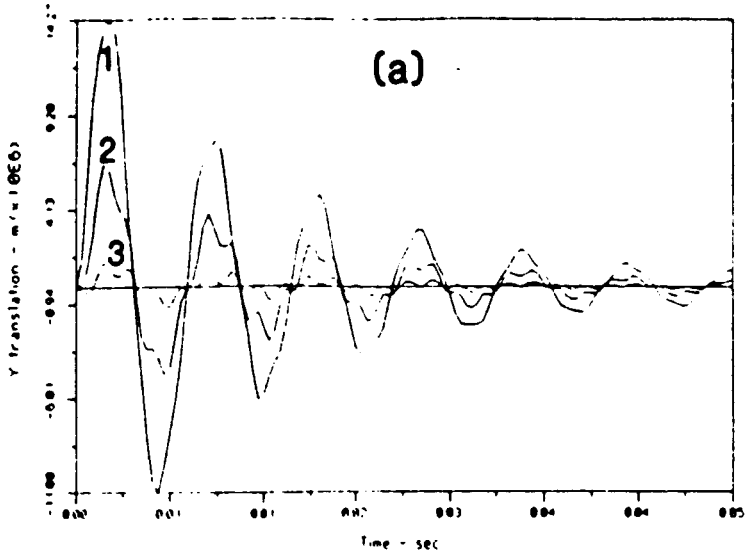

Figure (5-a) - Time response of steel cantilever beam controlled by one PZT actuator neglecting effect of bonding

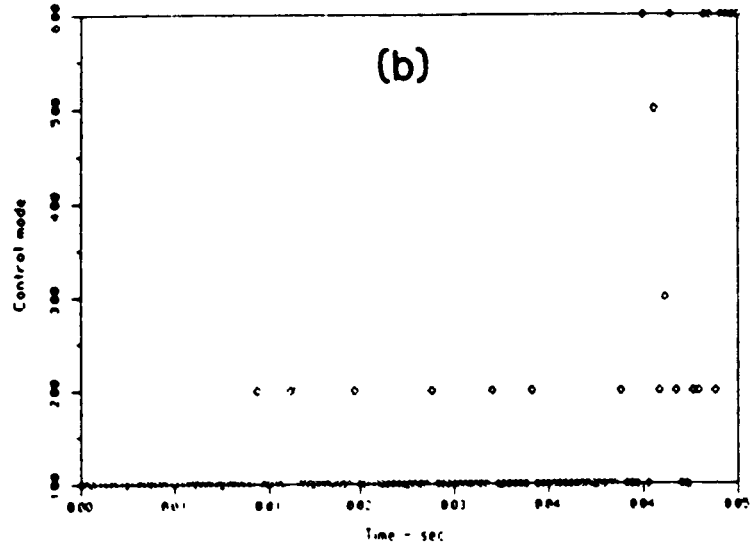

Figure (5-b) - Control mode of highest modal energy for the cantilever beam

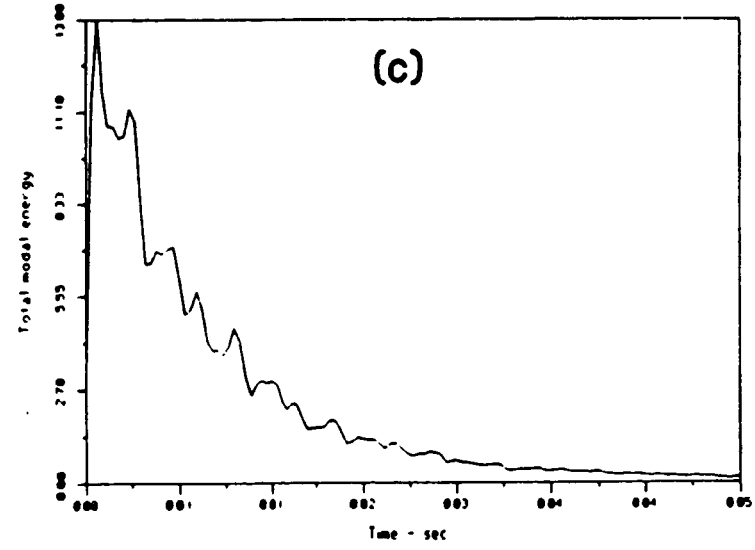

Figure (5-c) - Total modal energy of cantilever beam

(A) EFFECT OF BONDING LAYER THICKNESS

Figures (6-a), (6-b) and (6-c) display the time histories of the amplitudes of transverse vibrations of the cantilever beam when one PZT piezo-electric actuator is bonded to element 3 using an Isotac bonding layer of thickness of 0.42mm, 0.84mm and 2.1mm respectively. In dimensionless form, the selected bonding layers have thickness equal to 0.2, 0.4 and 1.0 that of the actuator thickness respectively.

A comparison between Figures (5-a) and (6-a) indicates that the maximum amplitude of vibration has decreased from 1.43E-5m to 1.39E-5m when the elastic and inertial properties of the bonding layer, that has a thickness of 0.00042m, are accounted for. Further decrease in the maximum amplitude of vibration is observed as the thickness of the bonding layer is increased as displayed in Figures (6-b) and (6-c).

Detailed analysis of the figures is summarized in Table (3) based on the displacement and control force indices U_d and U_c which are defined by the following expressions:

$$U_d = \sum_{t=0}^{t=t^*} \sum_{i=1}^{N} \delta_i^{2*} \Delta t \qquad (16)$$

$$U_c = \sum_{t=0}^{t=t^*} \sum_{i=1}^{N} F_i^{2*} \Delta t \qquad (17)$$

where N is the number of d.o.f. of system

Δt is the integration time increment

t^* is the maximum time limit of integration

Table (3) indicates clearly that including the effect of bonding layer results in decreasing the displacement index U_d monotonely but on

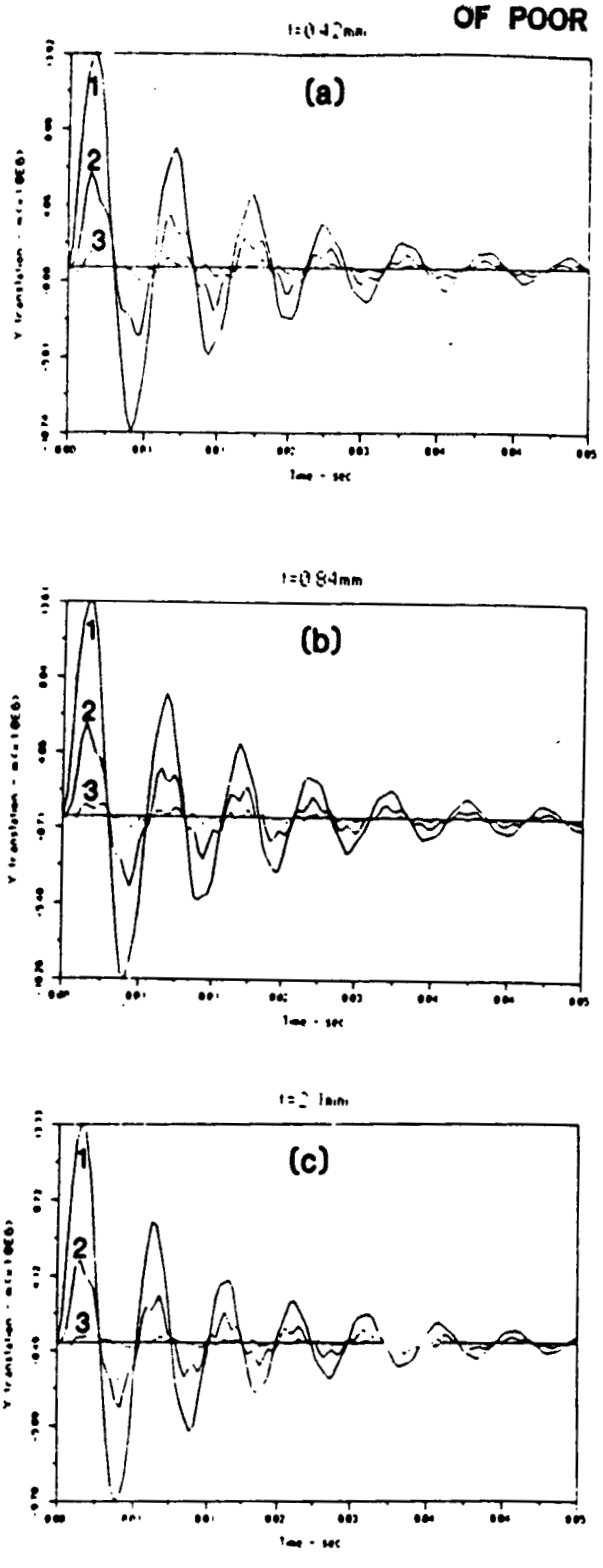

Figure (6) - Time response of steel cantilever beam controlled by one PZT actuator bonded to element 3 with Isotac of different thickness

Table (3) - Effect of bonding layer thickness on the displacement and control force indices for a steel cantilever beam controlled by one PZT actuator at element 3

Thickness (m)	Displacement index ($\times 10^{10}$)	Control force index ($\times 10^{7}$)
0	2.8244	1.8128
0.00042	2.6505	3.0164
0.00084	2.5531	3.4443
0.00210	2.3787	9.6501

the expense of a significant increase in the required control voltages. For example, using bonding layer thickness of 0.00042m reduces the displacement index from 2.8244E-10 to 2.6505E-10 whereas it increases the control force index from 1.8128E-7 to 3.0164E-7, which amount to an increase of 66%.

The reduction in the amplitudes of vibration of the beam resulting from using thicker bonding layers is attributed primarily to the stiffening effect produced by the bonding layers to the original actuator-beam system. However, using such thicker bonding layers would require large control forces to damp out the vibrations of the flexible beam. This is reflected directly into high control voltages as can be seen clearly from Figures (7-a), (7-b) and (7-c) for Isotac bonding layer thickness of 0.42mm, 0.84mm and 2.1mm respectively.

Therefore, we have a push and a pull situation where thicker bonding layer are preferred to minimize the amplitudes of oscillation and thinner bonding layers are desirable if one is to limit the magnitude of the control voltages.

(B) EFFECT OF BONDING LAYER MATERIAL

The effect of changing the material of the bonding layer from Isotac to Eastman 910 on the displacement and control force indices is summarized in Table (4). The results listed in the table are obtained when one PZT actuator is bonded to element 3 and a 0.42mm thick bonding layer is used.

Table (4) indicates that changing the bonding layer material from the soft Isotac to the more stiff and dense layer of Eastman 910 results in insignificant reduction in the displacement index but in a

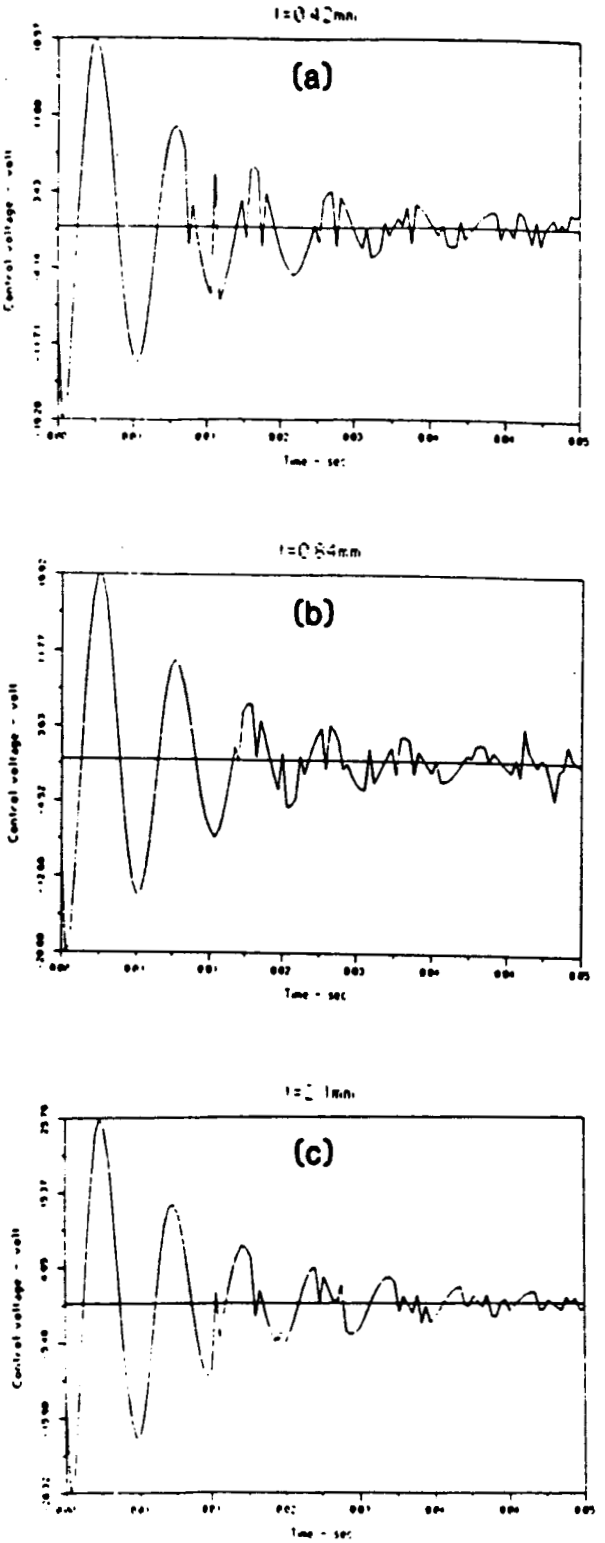

Figure (7) - Time history of voltage controlling a steel cantilever beam by one PZT actuator bonded to element 3 with Isotac of different thickness

Table (4) - Effect of bonding layer material on the displacement and control force indices for a steel cantilever beam controlled by one PZT actuator at element 3

Material	Displacement index ($\times 10^{10}$)	Control force index ($\times 10^{7}$)
Isotac	2.6505	3.0164
Eastman 910	2.6499	3.6320

considerable increase , of about 20.4%, in the forces necessary to control the vibration of the beam.

(C) EFFECT OF ACTUATOR LOCATION

Figures (8-a) and (8-b) show the time historIES of the amplitudes of transverse vibrations of the steel cantilever beam when a PZT actuator is bonded to element 2 and 3 respectively. The bonding layer considered, in this case, is Isotac which has a thickness of 0.00042m.

The associated displacement and control force indices are listed in Table (5).

Table (5) as well as Figures (5-a), (8-a) and (8-b) indicate that it is preferable to place the actuator at element 3 near the fixed end of the beam in order to obtain the minimum displacement index. On the other head, if the minimum control forces are concerned, then this actuator should bonded to element 1.

CONCLUSIONS

This paper has presented a comprehensive analysis of the control of vibration of simple structural elements using piezo-electric actuators. A Modified Independent Modal Space Control (MIMSC) method is utilized to actively control the vibration of the flexible system.

The effect of the physical parameters of the actuator and its bonding layer on the elastic and inertial characteristics of the flexible beam are included in the analysis. It is observed that accounting for the elastic and inertial properties of the bonding layer results in reducing

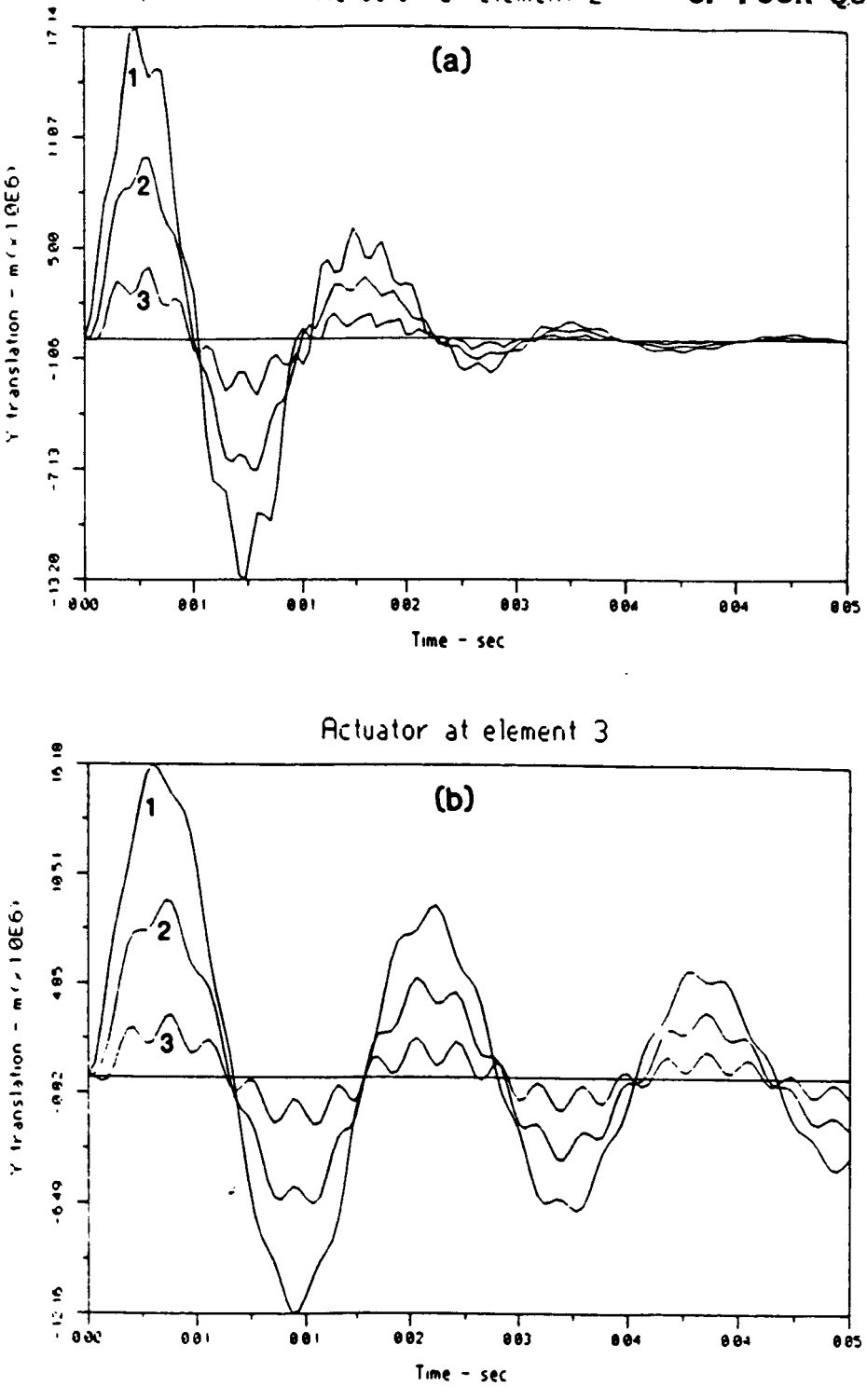

Figure (8) - Time response of steel cantilever beam controlled by one PZT actuator placed at different location

Table (5) - Effect of actuator location on the displacement and control force indices for a steel cantilever beam controlled with one PZT actuator

Actuator location	Displacement index ($x10^{10}$)	Control force index ($x10^{7}$)
Element 1	5.2855	0.1021
Element 2	3.3681	2.5494
Element 3	2.6505	3.0164

the amplitudes of vibrations of the structural element but on the expense of higher control forces.

The study has demonstrated also the effectiveness of the MIMSC method in controlling the vibration of flexible beams that have large number of degrees of freedom with very small number of actuators. Furthermore, the presented method can be readily extended to large structures without any modifications.

REFERENCES

1. Crawley, E.F., and J.de Luis 1985 Proc. of the 26th structures, Structure Dynamics and Materials conference, Part 2, AIAA-ASME-ASCE, Orlando-Florida, 126-133. Use of piezo-Ceramics as distributed actuators in Large Space Structures.
2. Bailey, T. and James E.Hubbard Jr. 1985 J. of Guidance and control 8 605-611. Distributed Piezo-electric Polymer Active Vibration Control of a Cantilever Beam.
3. Forward, R.L. 1981 J. Spacecraft 18 11-17. Electronic Damping of Orthogonal Bending Modes in a Cylindrical Mast-Experiment.
4. Lockheed Missiles and Space Company, Inc. 1983 VCOSS A: High and Low Authority Hardware Implementations Report #AFWAL-TR-83-3074. Vibration Control of Space Structures.
5. Aronson, R.B. 1984 Machine Design 56 73-77. Rediscovering Piezoelectrics.
6. Toda, M., S. Osaka and E. Johnson 1979 RCA Engineer 25 24-27. A new Electromotional Device.
7. Toda, M., S. Osaka and S. Tosima 1980 Ferroelectronics 23 115-120. Large Area Display Element Using PVF2 Bimorph With Double-Support Structure.
8. Piezo-Electric Products, Inc. 1984 Sensors Piezoceramic Design Notes.
9. Toda, M. 1978 Trans. of the IECE of Japan E61 507-512. Electromotional Device Using PVF2 Multilayer Bimorph.
10. Kelly Lee, J. and M. Marcus 1981 Ferroelectronics 32 93-101. The Deflection-Bandwidth Product of PVF Benders and Related Structures.
11. Toda, M. 1980 J. Appl. Phys. 51 4673-4677. Elastic Properties of

Piezo-Electric PVF2.

12. Baz, A. 1986 NASA Technical Report Contract No. 30429-D. Static Deflection Control of Flexible Beams by Piezo-Electric Actuators.

13. Meirovitch, L. and H. Baruh 1981 J. of Guidance and Control 4 157-163. Optimal Control of Damped Flexible Gyroscopic Systems.

14. Meirovitch, L. and H. Baruh 1982 J. of Guidance and Control 5 59-66. Control of Self-Adjoint Distributed-Parameter Systems.

15. Meirovitch, L., H. Baruh and H. Oz 1983 J. of Guidance and Control 6 302-310. Comparison of Control Techniques for Large Flexible Systems.

16. Baz, A. and S. Poh 1987 NASA Technical Report Contract No. 30429-D. Modified Independent Modal Space Control Method for Active Control of Flexible Systems.

17. Paz, M. 1985 Structural Dynamics : Theory and Computation 2nd Edition, Van Nostrand Reinhold Co, New York.

18. Bathe, K.J. and E.L. Wilson 1976 Numerical Methods in Finite Element Analysis Prentice-Hall Inc., Englewood Cliffs, NJ.

19. Fenner, R.T. 1975 Finite Element Methods for Engineers McMillan Press Ltd, Londan.

20. Gere, J.M and S.P. Timoshenko 1984 Mechanics of Materials 2nd Edition, Brooks/Cole Engineering Division, Monterey CA.

21. Meirovitch, L. 1967 Analytical Methods in Vibrations Macmillan Co., NY.